Effect of Spacer Length on the Specificity of Counterion-Cationic Gemini Surfactant Interaction

Rohit Sood[1], Juha-Matti Alakoskela[1], Anjali Sood[2], Pavol Vitovič[1,#] and Paavo K.J. Kinnunen[1,*]

[1]*Helsinki Biophysics and Biomembrane Group, Department of Biomedical Engineering and Computational Science, Aalto University, P.O.B. 12200, FIN-00076, Espoo, Finland*

[2]*Department of Chemistry, Laboratory of Inorganic Chemistry, Aalto University, P.O. Box 16100, FI-00076 Espoo, Finland*

Abstract: Aqueous solutions of three dicationic quaternary N,N-dimethylammonium gemini surfactants with identical hydrocarbon tails (N-hexadecyl) separated by flexible two, four, and six carbon atom spacers (di-, tetra-, and hexamethylene), abbreviated as G2, G4, and G6, respectively, were characterized using dynamic light scattering (DLS), Langmuir balance, differential scanning calorimetry (DSC), and microscopy in the presence of varying concentrations of sodium salts of fluoride, chloride, bromide, and iodide. Clear dependence on counterion species was evident in the surface activity of the geminis, as follows. In 0.1 mM salt minima in surface tension and hence presumably the highest affinity for G2, G4, and G6 were observed with fluoride/chloride, bromide, and iodide, respectively. This same ion specificity of G2, G4, and G6 was evident also in the changes of average hydrodynamic diameters (Z_{av}) with temperature. More specifically, maximum in Z_{av} for G2 was observed in 100 mM NaCl, for G4 in 100 mM NaBr, and for G6 in 1 mM NaI. Our results demonstrate that spacer length has a profound impact on interaction of these surfactants with halide counter-ions of different sizes, controlling organization of these cationic geminis in the presence of salt. Importantly, our studies show that adjusting the headgroup structure it is possible to design amphiphiles, which can be used to bind specific metal ions in solution, for purposes such as water purification and mineral enrichment.

Keywords: Gemini surfactants, counterions, spacer length, ion specificity, surface pressure.

INTRODUCTION

Gemini surfactants, composed of two conventional surfactants connected by a spacer [1-3], are an interesting class of amphiphilic molecules which demonstrate a number of properties uncommon for conventional surfactants, including very low CMCs, high surface activities, and rich pleomorphic phase behaviours [4-6]. They are efficient catalysts in organic reactions, possess high surface activity, and exhibit anomalous concentration-dependent viscosity changes, aggregation, and micelle structures. Their unusual amphiphilic characteristics make gemini surfactants cost-effective and environmental friendly alternatives to conventional surfactants [7]. The chemical structure of geminis allows for chemical synthesis of a great variety of different surfactants, thus making these amphiphiles particularly interesting for applications requiring precisely controlled self-assembly, such as lipofection [8, 9-11]. The most widely studied geminis are dicationic quaternary ammonium compounds, referred to as Cm-Cs-Cm, where m and s stand for carbon atom number of alkyl chains and methylene spacer, respectively [12].

Aqueous properties of surfactants such as micelle formation, aggregation, and degree of ionization are affected by additives such as aromatic acids/salts [13], nucleotides [14], polyelectrolytes [15], and counterions [16]. Of particular and long-standing interest have been ion-specific effects of counter-ions on surfactant and colloid properties, rationalized according to Hofmeister series. The physical basis of Hofmeister series remained unclear for a considerable time, however, ubiquitous ion-specific effects of Hofmeister series have been recently explained by effects of ion polarizability on their solvation free energy in aqueous solutions and on interactions with nonpolar surfaces. Ion-specific effects are well known from both biology and chemistry of chelators and ionophores, where specific distribution, chemical nature, and spacing of polar groups provides a high selectivity for specific ions. Recently, a novel mechanism allowing for specificity in ion interactions was suggested for a gemini surfactant with a rigid spacer. More specifically, commensurate lattice of charges in the presence of salt and gemini, resulting in surface crystallization of salt on gemini surface and leading to a sharp transition from micelles to giant vesicles to assemble into a nearly planar crystalline surface, enslaving surfactant

*Address corresponding to this author at the Department of Biomedical Engineering and Computational Science (BECS), Aalto University, Otakaari 3, FI-02150 Espoo, P. O. Box 12200, FI-00076 Aalto, Finland; Tel: + 358 50 5404600; Fax: + 358 9 4702 3182; E-mail: paavo.kinnunen@aalto.fi

#Current Address: Pavol Vitovic, Department of Nuclear Physics and Biophysics, Faculty of Mathematics, Physics and Computer Sciences, Comenius University, Mlynska Dolina F1, 842 48 Bratislava, Slovak Republic; E-mail: vitovic@cordbloodcenter.sk

E-ISSN: 1929-5030/12

membrane to the planar geometry favored by the ion-counterion lattice [7].

The spacer of a gemini surfactant can be rigid or flexible and to a varying degree hydrophilic, and is therefore expected to influence the aggregation properties, along with the length of hydrophobic tails. Further, spacer length also controls headgroup charge separation and chain packing [3]. In the present work, we studied specificity of counter-ion–gemini surfactant interactions with halides (*viz.* Na^+ salts of fluoride, chloride, bromide and iodide) and a series of dicationic quaternary ammonium gemini surfactants with flexible spacers of varying length. The studied cationic geminis have identical (C16) hydrocarbon tails with spacer lengths of 2, 4, and 6 carbon atoms. Interestingly, we observed a correlation between length of spacer and size of the counterion, evident in the self-assembly of these surfactants. At low salt and gemini concentrations the gemini with 2 carbon spacer showed strongest interaction with chloride, the gemini with 4 carbon spacer with bromide, and the gemini with 6 carbon spacer with iodide. The different salts also induced complex changes in the structure of gemini surfactant aggregates.

EXPERIMENTAL

Materials and Methods

NaF, NaCl, NaBr, NaI, NH_4Cl, NH_4Br, and NH_4I were from Sigma (Steinheim, Germany) and were used without further purification. Cationic gemini surfactants with identical hydrocarbon tails but different spacer lengths i.e. dimethylene-1,4-bis(N-hexadecyl-N,N-dimethylammonium bromide (G2), tetramethylene-1,4-bis(N-hexadecyl-N,N-dimethylammonium bromide (G4), and hexamethylene-1,6-bis(N-hexadecyl-N,N-dimethylammonium bromide (G6) (Figure **1**) were synthesized as described elsewhere [17] and their structures verified by NMR (200 MHz, Bruker, CA, USA). Concentrations of gemini surfactant stock solutions in chloroform were determined by gravimetric analysis [18] using a high precision electrobalance (SuperG; Kibron Inc, Espoo, Finland).

Surfactant Dispersions

Appropriate amounts of surfactant stock solutions were transferred into carefully cleaned test tubes and solvent was evaporated under a stream of nitrogen. Tubes were then sealed with parafilm and kept in vacuum overnight to remove any residual traces of solvent. The dry surfactant films were hydrated by deionised water (Milli RO, Millipore, Molsheim, France) or indicated salt solutions to yield a final surfactant concentration of 1 mM, followed by vigorous mixing and incubation for 45 min at 60 °C.

Surface Activity Measurements

Surface activity as a function of bulk concentration of G2, G4, and G6 in the presence of indicated concentrations of given salts, NaF, NaCl, NaBr, or NaI was measured. Dilution series of 11 concentrations of surfactants were prepared in disposable 96-well plates (Greiner Bio-One, Kremsmünster, Austria) using a multichannel pipette, with surfactant concentration given as $c \cdot x^{n-1}$, where x is the dilution factor (DF), c is the concentration of cationic gemini in column 1 (i.e. 1.0 mM), and n increases from 1 to 11, corresponding to columns 1 to 11 on the 96-well plate. For DF = 0.4, an aliquot of 70 µl was transferred from one column to consecutive one, up to column 11, with a total volume of 175 µl per well. Column 12 was filled with plain salt solution to provide a reference value for surface tension. Subsequently, 50 µl from each well was transferred into corresponding well of 96-well plate (Dyneplates, Kibron Inc., Helsinki, Finland) for measurement of surface tension. The plate was then covered with a lid, and allowed to equilibrate for 90 min prior to recording of surface tension [19-20] using an 8-channel surface tension microplate reader (Delta 8, Kibron Inc.). The instrument records value of surface tension by determining in triplicate maximum weight of meniscus adhering to a 0.5 mm diameter du Nouy probe upon its withdrawal from solution [21]. To minimize the impact of carry-over, plates were measured starting with column 12 containing salt solution without surfactant and then continuing towards increasing concentration of given gemini. The probes were automatically cleaned between each 96-well plate by heating in the built-in electric furnace of tensiometer.

Dynamic Light Scattering

Mean hydrodynamic diameters (Z_{av}, in nm) of gemini surfactants in the temperature range from 20 to 50 °C, both in water and with indicated salts were determined by photon correlation spectroscopy at a scattering angle of 173^0 (Zetasizer Nano ZS, Malvern Instruments Ltd., Malvern, UK). Surfactant dispersions (1 ml, final concentration 1 mM) were loaded into standard plastic cuvettes (Malvern) and measured twice at each temperature, controlled by the Peltier elements of instrument. Z_{av} was calculated from the diffusion coefficient (D) using Stokes-Einstein equation $Z_{av} = kT/3\pi\eta D$ where k is the Boltzmann coefficient, T

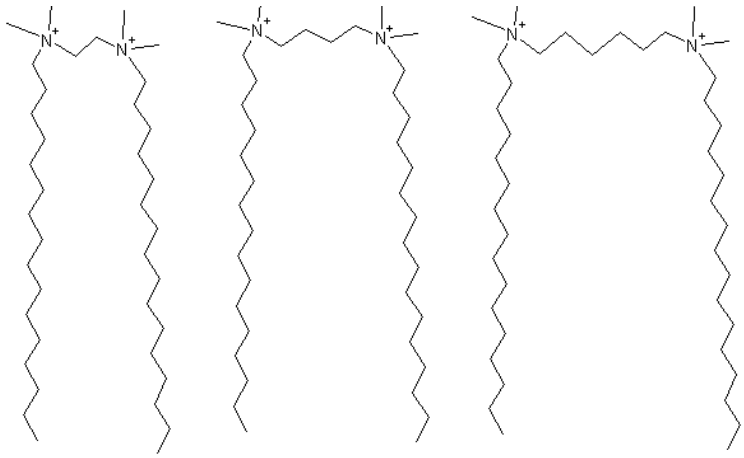

Figure 1: Structures of three cationic amphiphiles G2, G4, and G6 (from left to right) with identical hydrocarbon tails (C16) but differing in the lengths of their headgroup spacer.

the absolute temperature, and η viscosity of the solvent.

Differential Scanning Calorimetry (DSC)

After hydration surfactant dispersions (final concentration 1 mM) were vortexed and loaded into calorimeter cuvette. A VP–DSC microcalorimeter (Microcal Inc, Northampton, MA, USA) was operated at a heating rate of 0.5 degrees per minute and data were collected during heating scans from 10 to 70 °C. Phase transitions (T_m) were taken as temperatures at which endotherm reaches its maximum. The instrument was interfaced to a PC and data were analyzed using routines of the software provided by Microcal.

Optical Microscopy

An inverted microscope with differential interference optics (Olympus IX-70, Olympus, Tokyo, Japan) and with LCPlanFl 20x/0.40 objective was used for optical microscopy. The images were collected using a digital camera (D10, Canon Inc, Tokyo, Japan) attached to camera port of microscope. Surfactant suspension (1.5 ml) with indicated [salt] was applied into a chamber with quartz glass bottom, heated from 24 °C to 50 °C within approx. 50 min by a Peltier thermal microscopy stage (TS-4, Physitemp, Clifton, NJ, USA), monitoring temperature by an immersed Pt-100 probe (Omega, Stamford, CT, USA).

RESULTS

Solubility of G2, G4, and G6 in Different Salt Concentrations

Solubility of G2, G4, and G6 differed with different salt concentrations. G2, G4 and G6 were readily soluble in water as well as upto 100 mM of salt concentrations for NaF, NaCl, and NaBr. In the presence of NaI solubility of studied gemini's were quite low, for instance G2 and G4 was soluble in upto 40 mM NaI, however, G6 was least soluble in NaI and caused immediate precipitation at [NaI] > 1 mM. Hence due to this solubility problem we carried out surface pressure, DLS, and DSC experiments in the range of 0 to 100 mM for most of the compositions except in the presence of NaI, in this case working concentration was 0 to 1 mM.

Halide Anion Specificity for G2, G4, and G6 is Evident in their Surface Activity

Dependence of surface tension on the concentration of a surfactant yields adsorption isotherms revealing characteristic parameters such as critical micelle concentration (CMC), air/water partitioning coefficient (K_{aw}), and molecular cross sectional area (A_S). For these cationic gemini surfactants, however, the adsorption kinetics of surfactants at lower concentrations (0 to 1mM) was exceedingly slow, and equilibrium was not reached even after 4.5 h in repeated measurements. For even longer measurement times solvent under evaporation proved too significant for us to reach equilibrium. Hence, any estimates on CMC or molecular area we could present would be highly dependent on the time-point of measurement. In contrast, the maximal surface pressure of surfactants in the presence of different salts extracted from adsorption isotherms was nearly constant after 1.5 h.

Adsorption isotherms of G2, G4, and G6 were measured in the presence of Na^+ salts of F^-, Cl^-, Br^-,

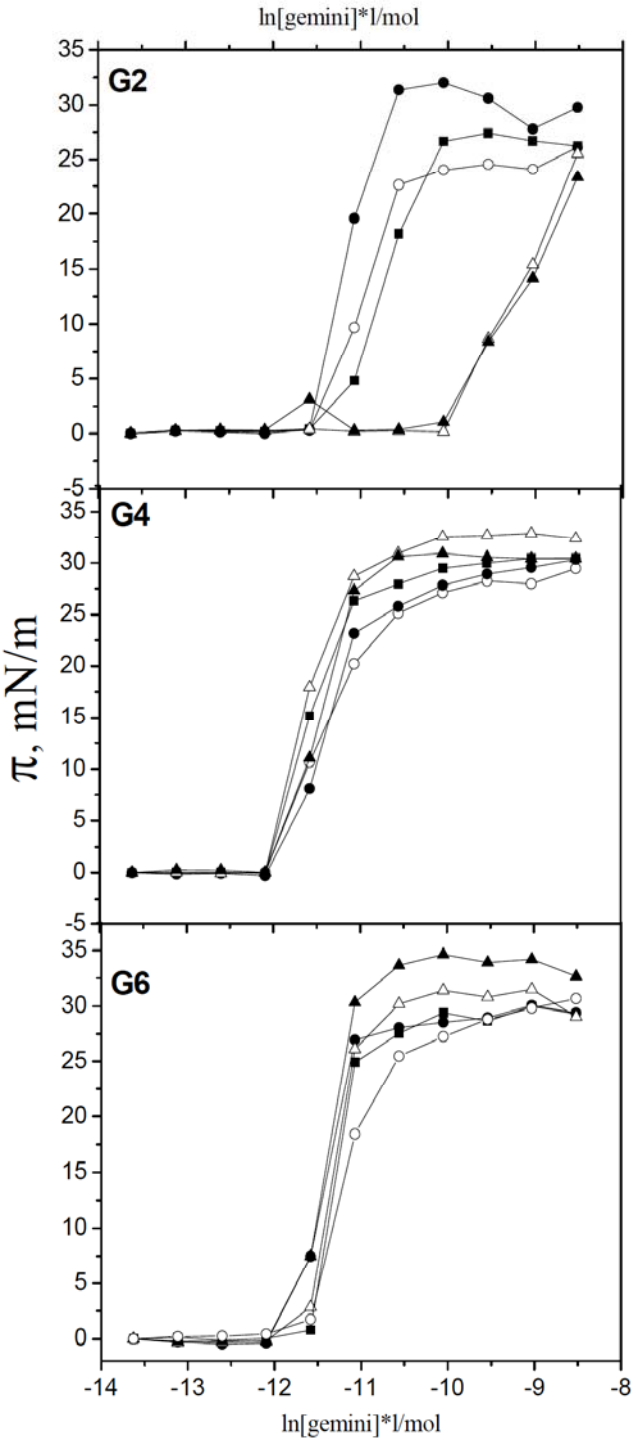

Figure 2: Surface pressure isotherms for G2, G4, and G6 (as indicated) in water (–), 0.1 mM NaF (,), NaCl (!), NaBr (8), and NaI (7).

and I^- (Figure **2**). For G2 maximum value of surface pressure (π_{max}) was higher in the presence of NaF and NaCl. Analogously, for G4 and G6 highest values of π_{max} were observed for NaBr and NaI (Figure **2**), respectively. Dependence of π_{max} for G2, G4, and G6 on counterion diameter at low [salt] = 0.1 mM was clearly seen (Figure **3**). Similar trend was observed at higher salt concentrations, but some of the surfactant–salt combinations precipitated at high salt concentrations, and hence we chose only low salt concentrations for comparison. Accordingly, maximum surface pressure, π_{max} and hence presumably highest affinity for G2, G4, and G6 was observed with fluoride and/or chloride, bromide, and iodide, respectively. The same ion specificity was evident in the CMC of surfactants at higher salt concentrations, with shifts to elevated values evident for ions as large or larger than chloride, bromide, or iodide, for G2, G4, and G6, respectively (data not shown).

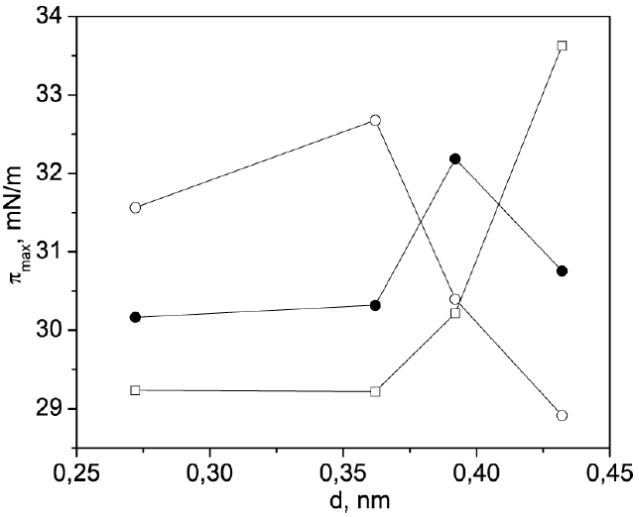

Figure 3: Variation of π_{max} measured in [salt] = 0.1 mM as a function of counterion diameter d, corresponding from left to right to F^-, Cl^-, Br^-, and I^- for G2 (–), G4 (,), and G6 (∀).

Effects of Temperature and Counterion on the Self-Assembly of G2, G4, and G6

DLS of three geminis, G2, G4, and G6 in the absence of salt gave average diameters, Z_{av} of 221, 167, and 164 nm, respectively, indicating the presence of small vesicles or clusters of micelles. A representative figure showing different transition phases observed during variation of Z_{av} with temperature for 1 mM G4 in the presence of 100 mM NaCl (Figure **4**, panel **A**) and NaBr (Figure **4**, panel **B**), respectively. Complete data set for variation of Z_{av} with temperature for different salt concentrations can be found in supplementary materials (Supporting Material, Figures **S1-S4**).

For G2 dispersions at [salt] = 0 mM Z_{av} increased linearly with temperature up to 30 °C, with a sharp decrease at T = 45 °C (Supporting Material, Figure **S1**, panel **A**). Temperature scans of aqueous dispersions

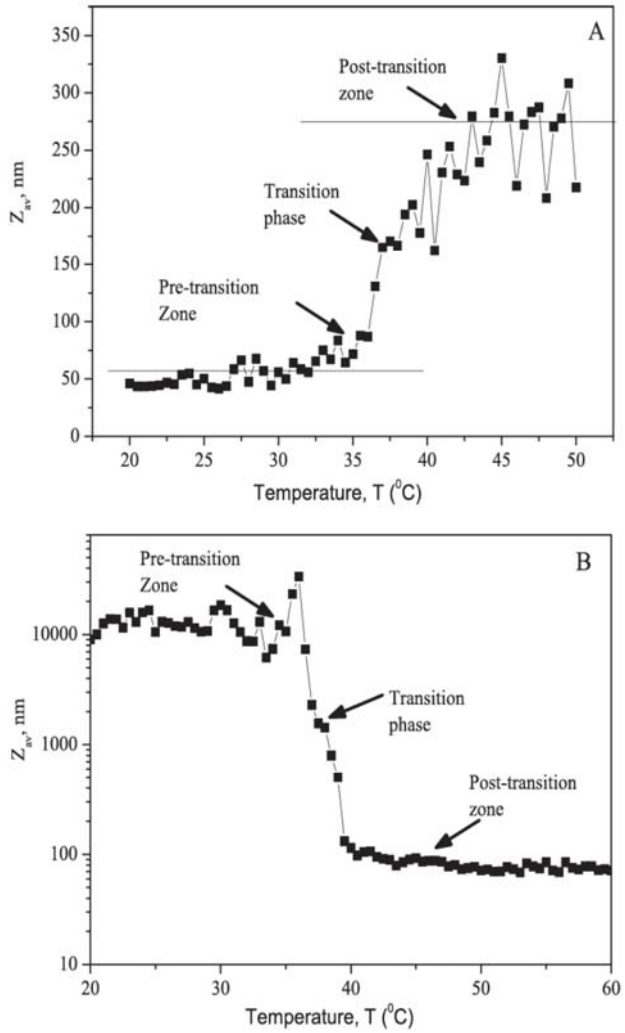

Figure 4: A representative figure showing variation of Z_{av} with temperature highlighting different transition phases for 1 mM G4 in the presence of 100 mM NaCl (panel **A**) and 100 mM NaBr (panel **B**), respectively.

of G4 at [salt] = 0 mM showed a progressive increase in Z_{av} from 165 to 700 nm (Supporting Material, Figure **S1**, panel **B**). G6 in the absence of salt and at room temperature had Z_{av} ≈ 164 nm, while with temperature Z_{av} increased to 2200 nm measured at 40 °C (Supporting Material, Figure **S1**, panel **C**). Subsequently, variation of Z_{av} with varying temperature was recorded for G2, G4, and G6 in the presence of different salt concentrations and Z_{av} was calculated for both pre and post transition periods and plotted vs [NaCl] (Figure **5**, panel **A**), [NaBr] (Figure **5**, panel **B**), and [NaI] (Figure **5**, panel **C**), respectively.

Most interesting changes in Z_{av} were observed for G2, G4, and G6 in the presence of NaCl, NaBr, and NaI, respectively, as the difference between pre and post transition Z_{av} was quite pronounced indicating strong interaction of counter ion Cl^-, Br^-, and I^- with two, four, and six carbon spacer of G2, G4, and G6, respectively.

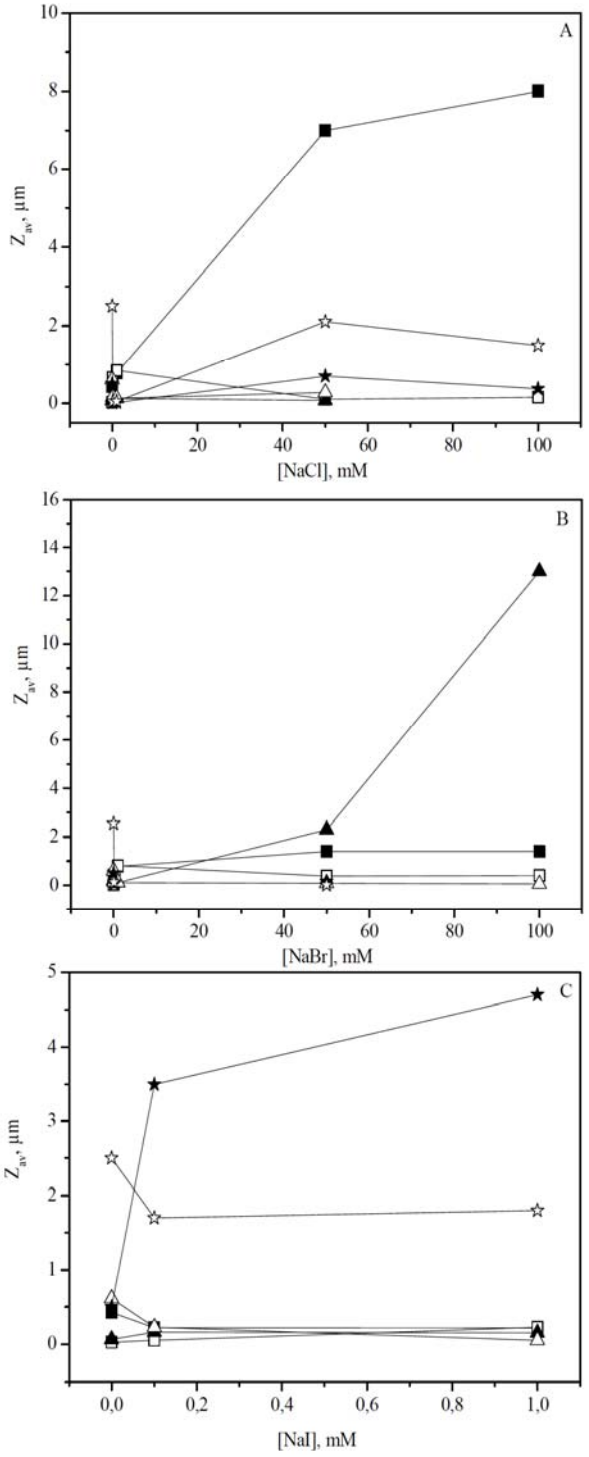

Figure 5: Pre (open symbols) and post transition (filled symbols) Z_{av} for G2 in 100 mM NaCl, for G4 in 100 mM NaBr, and for G6 in 1 mM NaI was calculated and plotted as a function of [salt]. Accordingly, variation of pre and post transition Z_{av} for G2 (□, ■), G4, (Δ,▲), and G6 (☆,★) in the presence of NaCl (panel **A**), NaBr (panel **B**), and NaI (panel **C**). Larger difference in the pre and post transition Z_{av} indicates higher affinity of gemini with counterion.

Transition temperatures obtained from DLS data were comparable to main phase transition temperature (T_m) observed in DSC scans. Accordingly, for aqueous dispersions of G2 three sharp endotherms following a minor peak at ≈ 36 °C were observed between 42 to 45 °C (Figure **6**, inset of panel **A**) whereas no endotherms were observed for dispersions of G4 and G6 in pure water. For G2 with 0.1 and 1 mM NaCl no significant shift in the endotherms was observed, however, with 50 mM NaCl, smaller peaks at 32 and 36 °C, preceded a large endotherm at ≈ 41 °C. The former smaller peaks were absent at [NaCl] = 100 mM while major peak remained. In the presence of 0.1 and 1 mM NaCl no endotherms were observed for aqueous dispersions of G4. But in 50 mM NaCl endotherm with T_m at ≈ 24 °C became evident for G4, further increase in [salt] had no significant effect (Figure **6**, panel **B**). For G6 up to 100 mM NaCl no endotherms were observed.

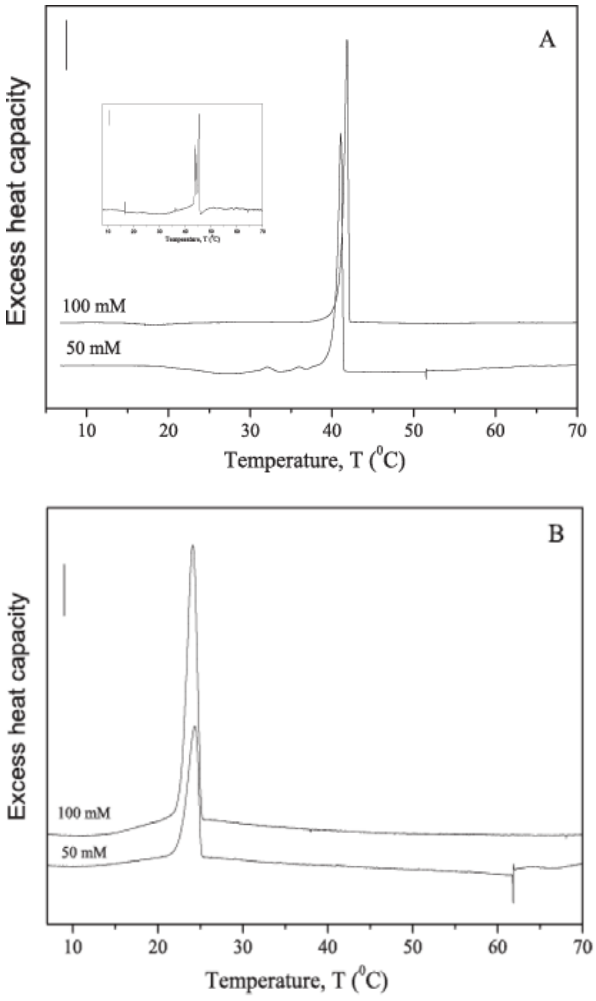

Figure 6: DSC traces of G2 (panel **A**), and G4 (panel **B**) in the presence of indicated [NaCl]. Dispersions of G2 in pure water exhibited a reproducible pattern of multiple endotherms (inset of panel **A**), whereas G4 in pure water did not exhibit any peak. No peak was observed for G6 either in the absence or presence of NaCl.

Variation of Z_{av} with temperature for G2 in the presence of 0.1 and 1 mM NaBr were identical to that in pure water and no endotherms were observed in DSC. In 50 mM NaBr Z_{av} for G2 increased with temperature reaching a maximum of 1500 nm at T = 43 °C, followed by a decrease in Z_{av} observed at ≈ 45 °C (Supporting Material, Figure **S3**, panel **A**). This transition is visible in DSC scans with sharp endotherm appearing at ≈ 45 °C (Figure **7**, panel **A**). No endotherms were observed for aqueous dispersions of G4 in the presence of 0.1 and 1.0 mM NaBr. However, DSC scans showed endotherm with T_m at ≈ 35.1 and 36.6 °C for G4 in 50 and 100 mM NaBr, respectively

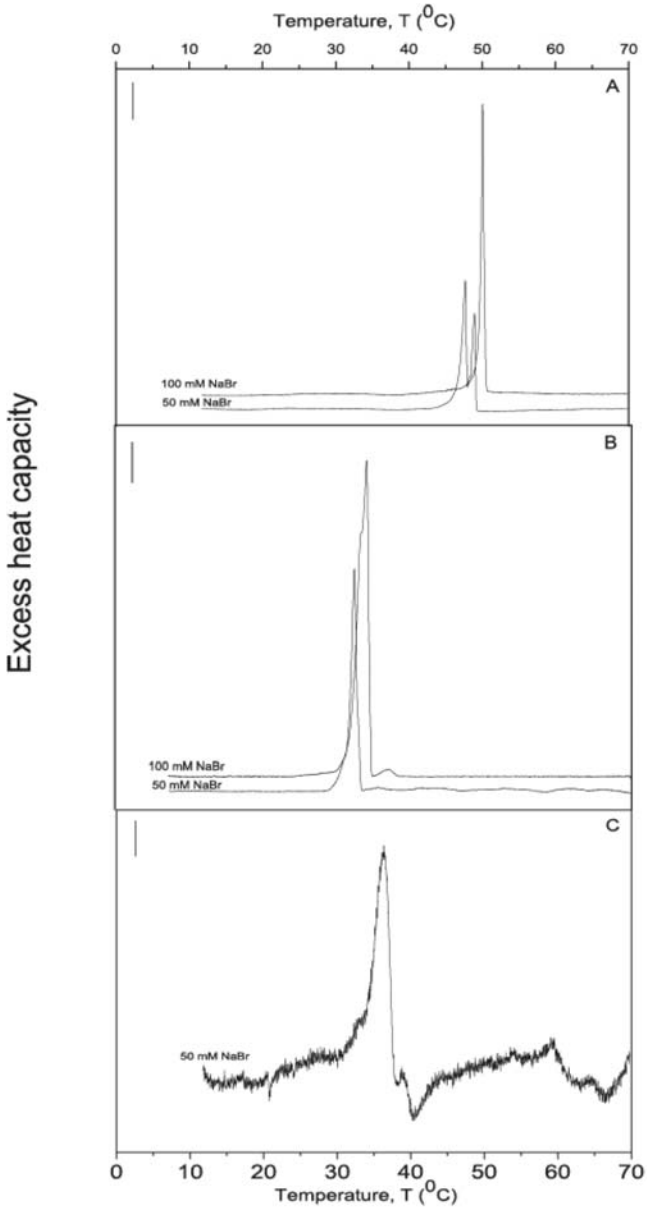

Figure 7: DSC traces of G2 (panel **A**), G4 (panel **B**), and G6 (panel **C**) in the presence of indicated [NaBr]. No endotherm was observed for G6 in the presence of 100 mM NaBr.

(Figure **7**, panel **B**). Values of T_m for G4 in the presence of NaBr were higher compared to NaCl indicating tighter packing. No endotherms were observed for aqueous dispersions of G6 in the presence of 0.1 and 1.0 mM NaBr. In 50 mM NaBr dispersions of G6 have $Z_{av} \approx 80$ nm at 20 °C, with increasing temperature augmenting Z_{av} up to 180 nm at 38 °C, followed by a drop result to $Z_{av} \approx 20$ nm at 41 °C (Supporting Material, Figure **S3**, panel **C**). In 50 mM NaBr DSC scans showed an endotherm at 35 °C (Figure **7**, panel **C**). Determination of Z_{av} and DSC scans was not possible to record due to precipitation of G6 in 100 mM NaBr.

DLS and DSC scans of G2 in the presence of 0.1 mM NaI exhibited transitions at 48 and 49 °C (Supporting Material, Figure **S4**, panel **A**), respectively, preceded by an additional minor peak at 38 °C (Supporting Material, Figure **S5**, panel **A**). In the presence of 1 mM NaI a sharp endotherm at 52 °C was observed (Supporting Material, Figure **S5**, panel **A**). No transition phase either in DSC or DLS was observed for G4 with 0.1 mM NaI whereas in 1 mM NaI DSC scan for G4 did show a broad endotherm ≈ 30 °C. In 0.1 mM NaI aqueous dispersions of G6 resulted in an increase in Z_{av} up to 3000 nm with a decrease in Z_{av} around 39 °C. In [NaI] = 1 mM Z_{av} increased to 4800 nm (Supporting Material, Figure **S4**, panel **C**). No endotherms were observed by DSC for G6 dispersions in the presence of NaI. The above findings are compiled into Table **1**.

In brief, thermal phase behavior and maximum in Z_{av} for three cationic geminis G2, G4, and G6 showed a strong dependence on the counterion. More specifically, maximum change in pre and post transition Z_{av} for G2 was observed in 100 mM NaCl (Figure **5**, panel **A**), for G4 in 100 mM NaBr (Figure **5**, panel **B**), and G6 in 1 mM NaI (Figure **5**, panel **C**).

Microscopy of Aggregates Formed by G2, G4, and G6

DLS revealed presence of large aggregates in the presence of salt for G2 and G4. To obtain better insight into the morphology of these aggregates, we imaged some of the large aggregates by optical microscopy. In particular, aqueous dispersions of G2, G4, and G6 with maximum increase in Z_{av} at particular [salt] were observed under optical microscope with temperature increased from 20 to 50 °C. Aggregates of varying morphologies were observed.

Dispersions of G4 in 100 mM NaBr appeared as free floating aggregates close to the bottom of the observation chamber at 25 °C (Figure **8**, panel **A**). Changes in morphologies of these aggregates were observed upon increasing the temperature to 30 °C. Occasionally, also large spherical vesicles were

Table 1: Maximum Apparent Values for Z_{av} (in nm) and T_m (Obtained from DSC) for G2, G4, and G6 in the Presence of Indicated Concentrations of NaCl, NaBr, and NaI, Respectively

	G2		G4		G6	
NaCl, mM	**Z_{av}**	**T_m**	**Z_{av}**	**T_m**	**Z_{av}**	**T_m**
0	221	45.3	700	NP*	2000	NP
0.1	800	45.1	155	NP	100	NP
1.0	900	45.0	130	NP	200	NP
50	7000	41.1	200	24.4	1000	NP
100	8000	41.2	150	24.1	800	NP
NaBr, mM						
0.1	145	NP	130	NP	200	NP
1.0	850	NP	150	NP		NP
50	1500	47.0	3000	35.0	200	35.0
100	2000	50.0	10000	36.0	150	PS*
NaI, mM						
0.1	250	45.0	150	30.0	3500	NP
1	300	50.0	150	30.0	4800	NP

NP* = No peak in DSC was observed.
PS* = Poor solubility.

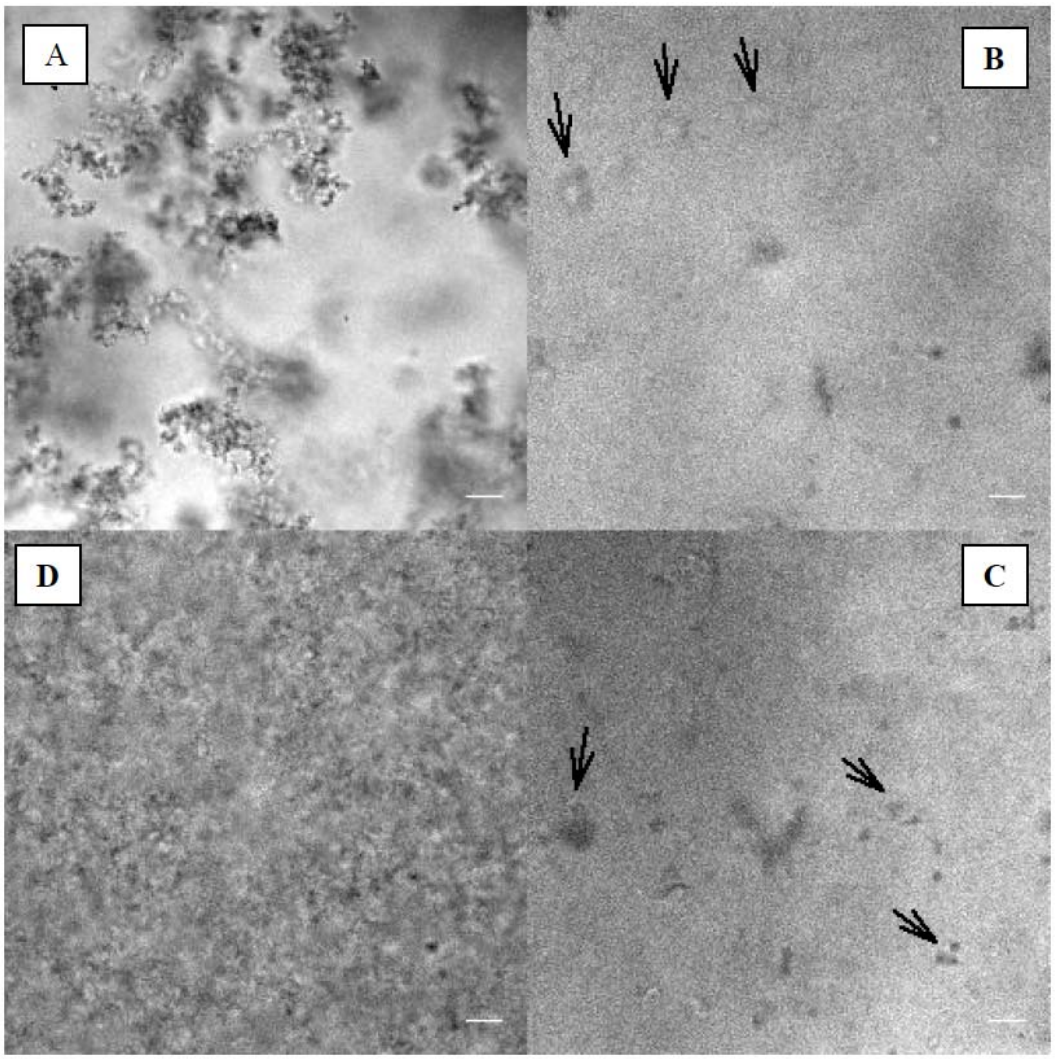

Figure 8: Visualization of aggregates formed by G2 and G4 in the presence of 100 mM NaCl and NaBr at different temperatures using optical microscopy. G4 in the presence of 100 mM NaBr at 25 °C (panel **A**), however, at 29 °C few large vesicles were seen (panel **B**), further heating to 40 °C leads to disappearance of larger vesicles yet smaller micelles were observed (panel **C**). Dense aggregates were observed for G2 in the presence 100 mM NaCl, morphology of these aggregates didn't changed with increase in temperature (panel **D**).

observed together with dense aggregates at ≈ 29 °C (Figure **8**, panel **B**). With increasing temperature up to 40 °C larger vesicles disappeared with the appearance of smaller vesicles (Figure **8**, panel **C**). In 100 mM NaCl the formation of dense aggregates by G2 was seen (Figure **8**, panel **D**). Their morphology did not change within the temperature range studied. For G6 in the presence of NaI no dense aggregates were observed. Overall size of the free floating aggregates formed by G6 (with NaI) was smaller (data not shown) compared to G2 (with NaCl) and G4 (with NaBr).

Effect of Temperature and Ammonium Salts on the Self-Assembly of G2, G4, and G6

In the commensurate lattice model not only identity of counterion but also identity of co-ion is expected to affect interactions of salt with surfactant. To check importance of the salt cation Z_{av} was measured also as a function of temperature for G2, G4, and G6 in the presence of NH_4Cl, NH_4Br, and NH_4I respectively. Most significant changes for G2 and G4 in the presence of NH_4Cl and NH_4Br were observed at concentrations ≥ 50 mM. Accordingly, in 100 mM NH_4Cl there was an increase in Z_{av} for G2 up to 2500 nm, with a transition at 41 °C (Figure **9**, panel **A**). This increase in Z_{av} was significantly less compared to the aqueous dispersions of G2 in the presence of NaCl. In 50 mM NH_4Cl a single peak at T_m ≈ 41.2 °C was observed in DSC and further increase to 100 mM NH_4Cl did not produce significant changes in T_m (data not shown). For G4 in 50 mM NH_4Br values of Z_{av} remain unchanged up to 30 °C, following an increase in Z_{av} up to 800 nm with a

transition at 35 °C. In 100 mM NH_4Br Z_{av} increased from beginning of the temperature scan with a maximum at 1000 nm followed by a transition around 36 °C (Figure **9**, panel **B**). DSC scans for aqueous dispersions of G4 in the presence of 50 and 100 mM NH_4Br resulted in T_m at ≈ 35.1 and 36.5 °C, respectively (data not shown).

Aqueous dispersions of G6 in the presence of 0.1 mM NH_4I resulted in slight increase in Z_{av} over the whole temperature range, however, it was not possible to record DLS/DSC scans at higher concentration of NH_4I due to poor solubility and immediate precipitation of G6.

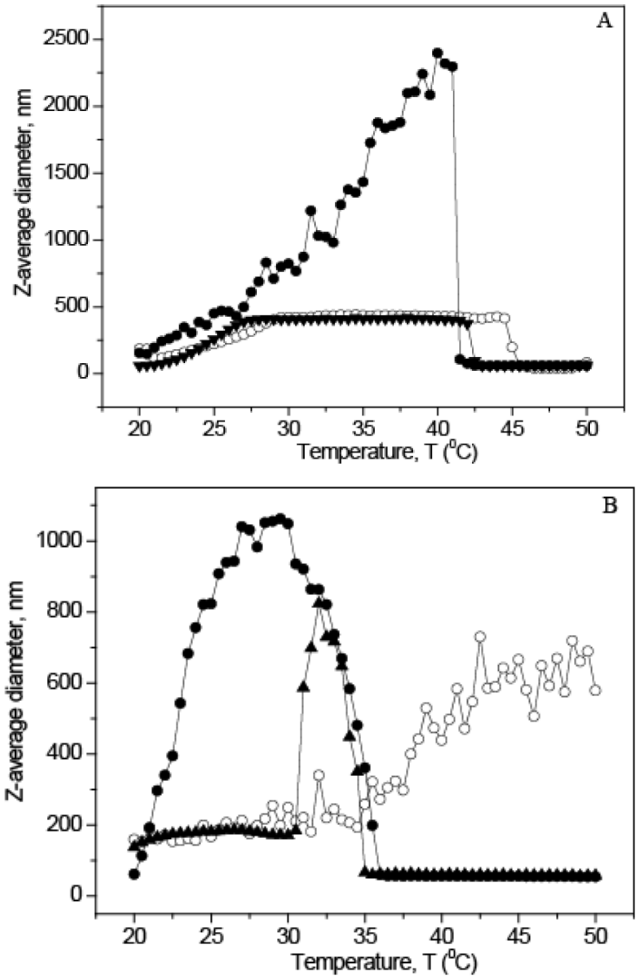

Figure 9: Variation of Z-average diameter *vs* temperature for one mM G2 (panel **A**) in the presence of [NH_4Cl] = 0 (–), 50 (B), and 100 mM (●) and for one mM G4 (panel **B**) in the presence of [NH_4Br] = 0 (–), 50 (B), and 100 mM (●).

DISCUSSION

Common effect of salt is to increase the melting temperature of charged amphiphiles. In gel-like phase headgroups are packed closer than in the fluid phase and when unscreened there is a strong repulsion between headgroups, favoring fluid phase, decreasing T_m. In contrast, presence of NaCl decreases T_m for aqueous dispersions of G2. One possibility is that in the absence of salt G2 is in interdigitated phase with a higher melting temperature [22] and that salt induced decrease in charge repulsion leads to the formation of a non-interdigitated state. The other possibility is that Cl^- ions binds with higher affinity to fluid phase G2, possibly requiring a headgroup conformation which is incompatible with gel phase packing. Addition of salt also results in disappearance of multiple components in the heat capacity scan with appearance of a single endotherm at 41 °C. The presence of multiple peaks in endotherms may derive from either different G2 aggregates morphologies (polymorphs) present in lipid membranes or from interdigitated → non-interdigitated transition followed by a chain melting transition. It seems that overall stability of assembly of G2 decreases in the presence of salt. This unusal behavior was further substantiated by measuring size of aggregates formed by G2 in the absence as well as presence of salt. It appears that within a particular temperature range and [NaCl] some kind of ion-counterion lattice is formed, which causes a large Z_{av} and it is thermally stable up to 40 °C. High specificity of G2 for Cl^- was observed also in surface activity measurements (Figures **2** and **3**). Transition temperatures obtained for G2 from DLS and DSC measurements are in good agreement with each other. Along similar lines, we have observed that gemini surfactant RR-1 interacts avidly with NaCl forming crystalline aggregates and suggesting specific interactions between RR-1 and Cl^-. We proposed that dicationic headgroup acts as a nucleating surface for Cl^- counterions to form a planar, pseudocrystalline lattice commensurate with 111-facet for Cl^- in a NaCl crystal [23]. In the present study, increase in spacer length results in increased distance between two headgroups preventing gel-like packing of surfactant molecules hence lacking a sharp melting transition with an observable enthalpy for aqueous dispersions of G4 and G6. However, 50 and 100 mM of NaCl was sufficient to screen highly charged headgroups of dicationic gemini, G4 and G6, leading to effective packing of surfactant molecules yielding endotherms at 24.4 and 30.4 °C, respectively. The order of stability in the presence of NaCl as reflected by T_m values from DSC was G2 > G6 > G4. Greater stability of G6 dispersions compared to G4 is interesting considering the fact that G6 has a longer spacer. Unusual thermal phase behavior (from DSC) and different kind of

aggregates formed (from DLS) by aqueous dispersions of G2, G4, and G6 in the absence as well as presence of [NaCl] prompted us to study effects of counter ions such as bromide and iodide. Interestingly, increase in T_m for dispersions of G2 in the presence of both NaBr and NaI could indicate absence of interdigitated phase (Figure **7**. panel **A** and Supporting Material, Figure **S5**, panel **A**), which was observed in the presence of NaCl. For dispersions of G4, an increase of ≈ 10 °C in T_m along with appearance of large aggregates indicates higher stability as well as high affinity of G4 for Br^- as a counterion. Upon comparison with I^- an increase by 4 °C of T_m and increase in Z_{av} upto ≈ 150 nm were observed. Similarly, high affinity of G6 for I^- as a counterion was observed whereas weaker interactions were observed for Cl^- and Br^-. The effects of different counterions was studied by measuring surface pressure as a function of surfactant concentration, yielding CMCs. We observed that spacer length controls the specificity for size of counter ion. For instance, G2 prefers fluoride and/or chloride, whereas G4 and G6 have high specificity for bromide and iodide as evidenced by higher values of π (at [salt] = 0.1 mM) and high CMCs (at [salt] > 20 mM).

We observed formation of dense aggregates for dispersions of G2 in NaCl (Figure **8**, panel **D**) and large aggregates for G4 in NaBr (Figure **8**, panels **A** & **B**). These aggregates of different morphologies could relate to headgroup-counterion hydration [22, 24] and molecular geometry of effective shapes of lipids controls 3-D phase behavior of lipid assemblies. This relationship is rationalized in terms of a packing parameter (p = υ/al) and for formation of planar bilayers (as observed in giant vesicles) p ≈ 1. For p ≈ 1 there should be significant reduction in the headgroup area leading to lower values of a. However, no evidence for reduction in a was obtained from DSC, since upon increasing [salt] slight increase in T_m was observed for these geminis indicating very little condensation of their aqueous dispersions. However, for dispersions of G2 in NaCl decrease in T_m was observed indicating expansion of bilayer. Recently, we have shown that a cationic gemini lipid M-1 undergoes a sharp transition from micelles to giant vesicles depending on NaCl concentration and temperature [7]. The headgroups of M-1 and G2, G4, and G6 are structurally very different with presence of chiral centers in the former. Hence extent of hydration of M-1 is likely to be different from G2, G4, and G6 and presence of counter ion will substantially alter it further leading to formation of aggregates of different morphologies.

It seems that fixed distance between dicationic head group of G2, G4, and G6 acts as a surface template for counterions to organize in a controlled fashion. Taking into account molecular parameters such as the length of $-(CH_2)_2-$, $-(CH_2)_4-$, $-(CH_2)_6-$ spacer in these geminis, ionic radii of different counterions with corresponding hydration shells it seems that Cl^- would match with spacer length of G2. Analogously, Br^- and I^- fit better with G4 and G6, respectively. Another evidence for counter ion size mismatch with spacer length of G4 and G6 was observed from DLS and DSC in the presence of NaCl. For instance, NaCl has no significant effect on T_m for aqueous dispersions of G4 while an increase of only 2.7 degrees in T_m for G6 was observed with continuous decrease in Z_{av} indicating less specificity for Cl^- counterion. Similar behavior was observed for G2 with Br^- and I^- and for G6 with Cl^- and Br^- as counterions. Upon replacing Na^+ with NH_4^+ much smaller aggregates of G2, G4, and G6 were observed. A likely reason for this difference for G2/G4/G6 with NaX salts (X = chloride/bromide/iodide) could be that dicationic headgroup acts as a nucleating surface for counterions to form a planar, commensurate pseudocrystalline lattice corresponding to 111-facet for NaX crystals and associated with vesicle surface. Next to this layer of X^- is Na^+, followed by another layer of X^-, and so on, thus promoting formation of large aggregates (evidenced by high Z_{av}). The ion-counterion lattice would form only after a threshold [NaX] reached at lower temperatures and is likely to be sensitive to the phase state of the nucleating membrane. More specifically, to efficiently initiate the formation of NaX crystal lattice, the amphiphiles in the bilayer would have to adapt their mean molecular area to lattice spacing. However, with $NH_4^+X^-$, due to mismatching of cation size in the second layer (and on subsequent cation layers) over the X^- layer would not be commensurate. This less favorable arrangement of ion-counterions imparts strain and/or little stability to overall structure preventing lattice to grow on top of dicationic headgroup leading to formation of much smaller aggregates (evidenced by smaller Z_{av}).

In the present study we show that specific length of an amphiphile is able to trap an ion of a particular size, for instance aqueous dispersions of G2, G4, and G6 are specific for Cl^-, Br^-, and I^-, respectively. Hence, our results shows that by carefully designing the head group structure, it could be possible to generate amphiphiles which can be used to bind specific metal ions in solution, for purposes such as water purification and mineral enrichment.

CONCLUSIONS

In continuation of our previous work [7], we have synthesized three cationic amphiphiles G2, G4, and G6 with alkyl spacers of two, four, and six carbon (Figure **1**) and studied their behavior in the presence of varying concentrations of sodium salts of fluoride, chloride, bromide, and iodide using DLS, Langmuir balance, DSC, and microscopy addressing importance of spacer length of headgroup in controlling interactions of these cationic gemini's with counterions. Although effects of salt on single tail surfactants such as alkyltrimethylammonium and alkylpyridinium are well documented [25-27], ion specificity of the corresponding gemini surfactants have not been explored in detail, though these interactions are likely to be important for their self-assembly and phase behaviour. Our results showed that length of spacer determines size specific interaction of cationic gemini with different counterions and fixed distance between dicationic head group of G2, G4, and G6 acts as a surface template for counterions to organize in a controlled fashion leading to formation of aggregates of different morphologies. A key consequence is that the counterion effects are specific beyond Hofmeister series and that also the co-ions induces co-ion specific changes in surfactant behavior. Further, our studies show that adjusting headgroup structure it is possible to generate amphiphiles which can be used to bind specific metal ions in solution, for purposes such as water purification and mineral enrichment.

ACKNOWLEDGEMENTS

HBBG is supported by Finnish Academy and Sigrid Juselius Foundation. RS was additionally supported by Paulo foundation.

SUPPORTING MATERIAL

The supporting material can be downloaded from the journal website along with the article.

REFERENCES

[1] Zana R. Dimeric (gemini) surfactants: effect of the spacer group on the association behavior in aqueous solution. J Colloid Interface Sci 2002; 248: 203-20. http://dx.doi.org/10.1006/jcis.2001.8104

[2] Menger F, Mbadugha BN. Gemini surfactants with a disaccharide spacer. J Am Chem Soc 2001; 123: 875-85. http://dx.doi.org/10.1021/ja0033178

[3] Grosmaire L, Chorro M, Chorro C, Partyka S, Zana R. Alkanediyl-alpha, omega-bis(dimethylalkylammonium bromide) surfactants 9. Effect of the spacer carbon number and temperature on the enthalpy of micellization. J. Colloid Interface Sci 2002; 246: 175-81. http://dx.doi.org/10.1006/jcis.2001.8001

[4] Menger FM, Keiper JS. Gemini surfactants. Angew Chem Int Ed 2000; 39: 1906-20. http://dx.doi.org/10.1002/1521-3773(20000602)39:11<1906::AID-ANIE1906>3.0.CO;2-Q

[5] Menger FM, Littau CA. Gemini surfactants: a new class of self-assembling molecules. J Am Chem Soc 1993; 115: 10083-90. http://dx.doi.org/10.1021/ja00075a025

[6] Menger FM, Littau CA. Gemini-surfactants: synthesis and properties. J Am Chem Soc 1991; 113: 1451-2. http://dx.doi.org/10.1021/ja00004a077

[7] Ryhänen SJ, Säily VM, Parry MJ, *et al*. Counterion-controlled transition of a cationic gemini from submicroscopic to giant vesicles. J Am Chem Soc 2006; 128: 8659-63. http://dx.doi.org/10.1021/ja060382u

[8] Kirby AJ, Camilleri P, Engberts JBFN, *et al*. Gemini surfactants: new synthetic vectors for gene transfection. Angew Chem Int Ed 2003; 42: 1448-57. http://dx.doi.org/10.1002/anie.200201597

[9] Badea I, Verrall R, Estrada MB, *et al*. *In vivo* cutaneous interferon-gamma gene delivery using novel dicationic (gemini) surfactant-plasmid complexes. J Gene Med 2005; 7: 1200-14. http://dx.doi.org/10.1002/jgm.763

[10] Badea I, Wettig S, Verrall R, Foldvari M. Topical non-invasive gene delivery using gemini nanoparticles in interferon-gamma-deficient mice. Eur J Pharm Biopharm 2007; 65: 414-22. http://dx.doi.org/10.1016/j.ejpb.2007.01.002

[11] Ryhänen SJ, Säily MJ, Paukku T, *et al*. Surface charge density determines the efficiency of cationic gemini surfactant based lipofection. Biophys J 2003; 84: 578-87. http://dx.doi.org/10.1016/S0006-3495(03)74878-4

[12] Zana R. Dimeric and oligomeric surfactants. Behavior at interfaces and in aqueous solution: a review. Adv Colloid Inter Sci 2003; 97: 205-53. http://dx.doi.org/10.1016/S0001-8686(01)00069-0

[13] Kabir-ud-Din FW, Khan ZA, Dar AA. ^{1}H NMR and viscometric studies on cationic gemini surfactants in presence of aromatic acids and salts. J Phys Chem B 2007; 111: 8860-7. http://dx.doi.org/10.1021/jp070782j

[14] McLoughlin D, Delsanti M, Albouy MPA, Langevin D. Aggregates formation between short DNA fragments and cationic surfactants. Mol Phys 2005; 103: 3125-39. http://dx.doi.org/10.1080/00268970500250460

[15] Goddard ED. Polymer/Surfactant Interaction: Interfacial Aspects. J Colloid Inter Sci 2002; 256: 228-35. http://dx.doi.org/10.1006/jcis.2001.8066

[16] Jianga N, Lib P, Wanga Y. Aggregation behavior of hexadecyltrimethylammonium surfactants with various counterions in aqueous solution. J Colloid Inter Sci 2005; 286: 755-60. http://dx.doi.org/10.1016/j.jcis.2005.01.064

[17] Zana R, Benrraou M, Rueff R. Alkanediyl-.alpha.,.omega.-bis(dimethylalkylammonium bromide) surfactants. 1. Effect of the spacer chain length on the critical micelle concentration and micelle ionization degree. Langmuir 1991; 7: 1072-75. http://dx.doi.org/10.1021/la00054a008

[18] Tejera-Garcia R, Connell L, Shaw WA, Kinnunen PKJ. Gravimetric determination of phospholipid concentration. Chem Phys Lipids 2012; 6: 689-95. http://dx.doi.org/10.1016/j.chemphyslip.2012.06.005

[19] Vitovič P, Alakoskela JM, Kinnunen PKJ. Assessment of drug-lipid complex formation by a high-throughput Langmuir-

balance and correlation to phospholipidosis. J Med Chem 2008; 51: 1842-48. http://dx.doi.org/10.1021/jm7013953

[20] Suomalainen P, Johans C, Soderlund T, Kinnunen PKJ. Surface activity profiling of drugs applied to the prediction of blood-brain barrier permeability. J Med Chem 2004; 47: 1783-88. http://dx.doi.org/10.1021/jm0309001

[21] Padday JF, Pitt AR, Pashley RM. Menisci at a free liquid surface: Surface tension from the maximum pull on a rod. J Chem Soc Fr 1 1974; 71: 1919-31.

[22] Ryhänen SJ, Alakoskela JM, Kinnunen PKJ. Increasing surface charge density induces interdigitation in vesicles of cationic amphiphile and phosphatidylcholine. Langmuir 2005; 21: 5707-15. http://dx.doi.org/10.1021/la0503303

[23] Ryhänen SJ, Säily VMJ, Kinnunen PKJ. Cationic lipid membranes-specific interactions with counter-ions. J Phys Condens Matter 2006; 18(28): S1139-50. http://dx.doi.org/10.1088/0953-8984/18/28/S03

[24] Geng Y, Romstead SL, Menger F. Specific ion pairing and interfacial hydration as controlling factors in gemini micelle morphology. Chemical trapping studies. J Am Chem Soc 2006; 128: 492-501. http://dx.doi.org/10.1021/ja056807e

[25] Knock MM, Main CD. Effect of counterion on monolayers of hexadecyltrimethylammonium halides at the air−water interface. Langmuir 2000; 16: 2857-65. http://dx.doi.org/10.1021/la991031e

[26] Subramanian V, Ducker WA. Counterion effects on adsorbed micellar shape: experimental study of the role of polarizability and charge. Langmuir 2000; 16: 4447-54. http://dx.doi.org/10.1021/la991245w

[27] Bijma K, Engberts JBFN. Effect of counterions on properties of micelles formed by alkylpyridinium surfactants. 1. conductometry and ^{1}H-NMR chemical shifts. Langmuir 1997; 13: 4843-49. http://dx.doi.org/10.1021/la970171q

Received on 19-09-2012 Accepted on 02-10-2012 Published on 15-10-2012

DOI: http://dx.doi.org/10.6000/1929-5030.2012.01.01.3